Sound Propagation in a Uniform Superfluid Two-Dimensional Bose Gas

J. L. Ville, R. Saint-Jalm, É. Le Cerf, M. Aidelsburger, S. Nascimbène, J Dalibard, J. Beugnon

Sound propagation in a uniform superfluid two-dimensional Bose gas

J.L. Ville, R. Saint-Jalm, É. Le Cerf, M. Aidelsburger[†], S. Nascimbène, J. Dalibard, and J. Beugnon[*]
[1] *Laboratoire Kastler Brossel, Collège de France, CNRS, ENS-PSL University, Sorbonne Université, 11 Place Marcelin Berthelot, 75005 Paris, France*

(Dated: August 30, 2018)

In superfluid systems several sound modes can be excited, as for example first and second sound in liquid helium. Here, we excite running and standing waves in a uniform two-dimensional Bose gas and we characterize the propagation of sound in both the superfluid and normal regimes. In the superfluid phase, the measured speed of sound is in good agreement with the prediction of a two-fluid hydrodynamic model, and the weak damping is well explained by the scattering with thermal excitations. In the normal phase we observe a stronger damping, that we attribute to a departure from hydrodynamic behavior.

Propagation of sound waves is at the heart of our understanding of quantum fluids. In liquid helium, the celebrated two-fluid model was confirmed by the observation of first and second sound modes [1, 2]. There, first sound stands for the usual sound appellation, namely a density wave for which normal and superfluid fractions oscillate in phase. Second sound corresponds to a pure entropy wave with no perturbation in density (normal and superfluid components oscillating out of phase), and is generally considered as a smoking gun of superfluidity.

Sound wave propagation is also central to the study of dilute quantum gases, providing information on thermodynamic properties, relaxation mechanisms and superfluid behavior. In ultracold strongly interacting Fermi gases, the existence of first and second sound modes in the superfluid phase was predicted [3] and observed in experiments [4, 5], with a behavior similar to liquid helium. In three-dimensional (3D) weakly interacting Bose-Einstein condensates (BECs), one still expects two branches of sound with speeds $c^{(1)} > c^{(2)}$ but the nature of first and second sound is strongly modified because of their large compressibility [6]. At zero temperature the gas is fully superfluid and the only relevant mode corresponds to Bogoliubov excitations, *i.e.*, density oscillations. At non-zero temperature, an isothermal density perturbation is expected to excite mostly the second sound mode, propagating at a velocity approximately proportional to the square root of the superfluid fraction [6, 7]. This contrasts to the usual picture for liquid helium where second sound is excited via local heating [1, 2]. Sound waves in an elongated 3D BEC were observed in Refs. [8–10] in a regime where the sound speed remains close to the Bogoliubov sound speed.

The study of sound propagation can be very insightful for two-dimensional (2D) Bose fluids, where superfluidity does not result from a Bose-Einstein condensation, but occurs instead via a Berezinskii-Kosterlitz-Thouless (BKT) transition [11]. This transition is associated with a jump of the superfluid density but as the transition is of infinite order, the jump cannot be revealed by the thermodynamic properties of the fluid. However, the presence of a superfluid component is predicted to lead to two distinct sound modes, whose velocities $c_{\mathrm{HD}}^{(1)}$ and $c_{\mathrm{HD}}^{(2)}$ were calculated within a hydrodynamic model in Refs. [12, 13]. These velocities are functions of the superfluid density and thus both exhibit a discontinuity associated with the superfluid jump at the critical point. In particular the second sound velocity is expected to remain non-zero just below the critical point of the superfluid to normal transition and to disappear just above. Experimentally, 2D Bose fluids were first realized with liquid helium films adsorbed on a substrate [14]; in this case the presence of the substrate blocks the motion of the normal component and thus prevents the investigation of such phenomena.

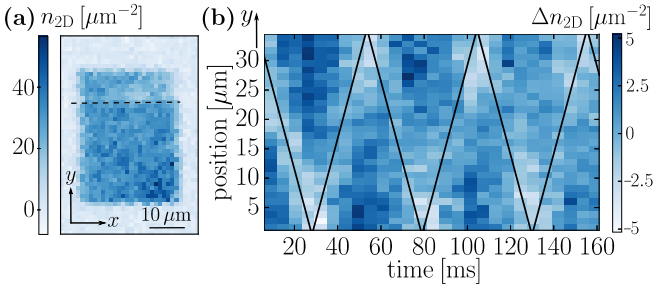

FIG. 1. Experimental protocol and observation of propagating waves. (a) Absorption image of the cloud perturbed by a local additional potential. The excitation is delimited by the horizontal dashed line and depletes the atomic density by a factor around 1/3. (b) Example of time evolution of the variation of the density profile n_{2D} with respect to its spatial mean value (integrated along x) obtained after abruptly removing the additional potential. For this example $T/T_c = 0.37(12)$ and $n_{2D} = 29(3)$ µm^{-2}. The position of the dip is fitted by a triangle function (black solid line) which gives, c =1.49(3) mm/s.

In this Letter, we report on the first observation of sound propagation in a 2D Bose fluid. We observe a single density sound mode both in the superfluid and normal regimes. Deep in the superfluid regime, the measured sound speed agrees well with the Bogoliubov prediction. We measure a weak damping rate compatible with Landau damping, a fundamental mechanism for the understanding of collective modes of superfluids at finite temperature [15]. For higher temperatures, we observe a

decrease of the sound velocity consistent with the second sound speed variation predicted in Ref. [12] from two-fluid hydrodynamics. The damping of sound increases with temperature and, above the critical point, we still observe strongly damped density waves with no discernable discontinuity at the critical point. The discrepancy with the two-fluid model predictions could be due to a departure from hydrodynamic behavior.

Our experimental setup has been described in Refs [16, 17] and more details can be found in [18]. Briefly, we confine ^{87}Rb atoms in the $|F = 1, m = 0\rangle$ ground state into a 2D rectangular box potential of size $L_x \times L_y = 30(1) \times 38(1)$ µm (see Fig. 1a). The confinement along the vertical z direction can be approximated by a harmonic potential of frequency $\omega_z/(2\pi) = 4.59(4)$ kHz. We always operate in the quasi-2D regime where interaction and thermal energies are smaller than $\hbar\omega_z$. The gas is characterized by the effective coupling constant $g = \hbar^2\tilde{g}/m = (\hbar^2/m)\sqrt{8\pi}\, a_s/\ell_z$, where a_s is the s-wave scattering length, $\ell_z = \sqrt{\hbar/(m\omega_z)}$ and m the atomic mass [11]. We operate here in the weakly-interacting regime: $\tilde{g} = 0.16(1)$. In the quasi-2D regime and for a given $\tilde{g}$, the equilibrium state of the cloud is only characterized by a dimensionless combination of T and n_{2D}, thanks to an approximate scale-invariance [11]. In the following we use the ratio T/T_c, where $T_c = 2\pi n_{2D}\hbar^2/[mk_B \ln(380/\tilde{g})]$ is the calculated critical temperature for the BKT phase transition [19]. In this work, we study Bose gases from the highly degenerate regime ($T/T_c \approx 0.2$) to the normal regime ($T/T_c \approx 1.4$).

We first investigate propagating waves which we excite by a density perturbation. Prior to evaporative cooling in the box potential, we apply to the cloud a repulsive potential, which creates a density dip on one side of the rectangle (see Fig. 1a). The extension of this dip is about 1/4 of the length of the box and its amplitude is chosen so that the density in this region is decreased by a factor of 1/3. After equilibration, we abruptly remove the additional potential and monitor the propagation of this density dip. We show in Fig. 1b a typical time evolution of the density profile integrated along the transverse direction to the perturbation for a strongly degenerate gas. In this regime, the density perturbation propagates at constant speed and bounces several times off the walls of the box. Using the calibrated size of the box, we extract a speed $c = 1.49(3)$ mm/s. This value is slightly lower than the Bogoliubov sound speed $c_B = \sqrt{gn_{2D}/m} = 1.6(1)$ mm/s expected at zero temperature for the measured density $n_{2D} = 29(3)$ µm^{-2}. The measured speed is also close to the second sound mode velocity $c_{HD}^{(2)} = 1.4(1)$ mm/s, estimated from two-fluid hydrodynamics at our experimental value of $T/T_c = 0.37(12)$ [12]. The first sound, expected to propagate at a much higher speed $c_{HD}^{(1)} = 3.3(3)$ mm/s [12], does not appear in our measurements that feature a single wavefront only. The absence of first sound in our experiments can be explained by its very small coupling to isothermal density excitations in a weakly interacting gas [12].

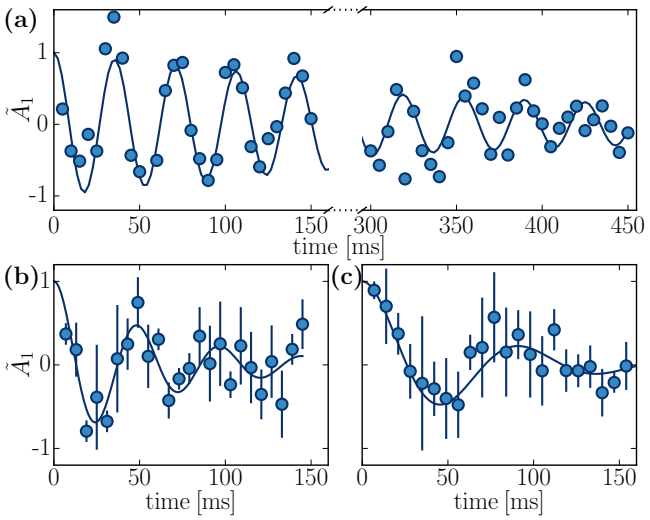

FIG. 2. Time evolution of the normalized amplitude of the lowest-energy mode for (a) $T/T_c = 0.21(11)$, (b) $T/T_c = 0.95(5)$, (c) $T/T_c = 1.38(18)$. The solid line is a fit of an exponentially damped sinusoidal oscillation. For (b) and (c) graphs, each data point is the average of three measurements and the error bars represent the associated standard deviation. In (a) each point corresponds to a single measurement.

In order to probe the role of the cloud degeneracy on the sound wave propagation, we vary both n_{2D} and T. For each configuration, we excite the cloud with the protocol described above, while adjusting the intensity of the depleting laser beam to keep the density dip around 1/3 of non-perturbed density. At lower degeneracies, sound waves are strongly damped and the aforementioned measurements of the density dip position become inadequate. We thus focus on the time evolution of the lowest-energy mode [20]. We decompose the density profiles integrated along x as

$$n(y,t) = \bar{n} + \sum_{j=1}^{\infty} A_j(t)\, \cos(j\pi y/L_y), \qquad (1)$$

where $\bar{n}$ is the average density along y and the A_j are the amplitudes of the modes. The choice of the cosine basis ensures the cancellation of the velocity field on the edges of the box. Our excitation protocol mainly couples to the lowest energy modes. We keep the excitation to a low value to be in the linear regime while still observing a clear signal for the lowest-energy mode, which in return provides a too weak signal for a quantitative analysis of higher modes [21]. For each duration of the evolution, we compute the overlap of the atomic density profile with the lowest-energy mode. Examples of the time evolution of the normalized amplitude $\tilde{A}_1(t) = A_1(t)/A_1(0)$ for differ-

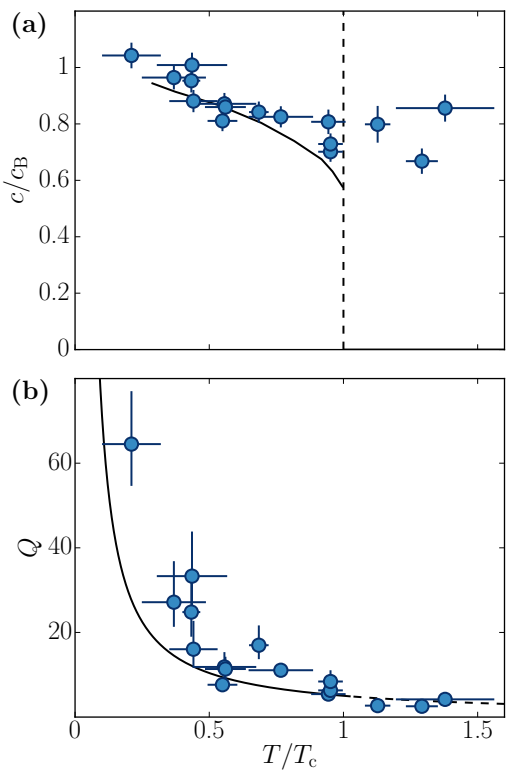

FIG. 3. Speed of sound and quality factor. (a) Measured speed of sound c normalized to c_B. The vertical dashed line shows the position of the critical point. The solid line shows the result from the two-fluid hydrodynamic model applied to the 2D Bose gas [12]. A fit to the data points below T_c by this hydrodynamic model with a free multiplicative factor shows that the measurements are globally 3% above the theoretical prediction. This could correspond to a 6% systematic error in the calibration of n_{2D} used to determine $c_B \propto n_{2D}^{1/2}$. Our estimated uncertainty on n_{2D} is on the order of 11% (see Ref. [18]) and our measurements are thus compatible with the predicted value of the speed of second sound $c_{HD}^{(2)}$. (b) Quality factor $Q = 2\omega/\Gamma$ of the lowest-energy mode. The solid line is the prediction for Landau damping [23] (continued as a dashed line for $T > T_c$). For both graphs, the error bars represent the statistical uncertainty extracted from the fitting procedures used to determine c, Γ and T/T_c.

ent degrees of degeneracy are shown in Fig. 2. We observe damped oscillations with a damping rate increasing with T/T_c. We fit the experimental data by an exponentially damped sinusoidal curve $e^{-\Gamma t/2}[\Gamma/2\omega \sin(\omega t)+\cos(\omega t)]$ to determine the energy damping rate Γ and the frequency ω [22]. We then determine the speed of sound $c = L_y\omega/\pi$ and the quality factor of this mode $Q = 2\omega/\Gamma$.

We consolidate all our measurements of speed of sound and quality factors in Fig. 3. To facilitate comparison with theory, we show in Fig. 3a the values of c normalized to c_B. The non-normalized results are reported in Ref. [18] for completeness. In the temperature range $T \lesssim 0.9\,T_c$, we measure weakly damped density oscillations, corresponding to a well-defined sound mode ($Q \gtrsim 10$). In this regime, we observe a significant decrease by about $\approx 25\%$ of the sound velocity for increasing values of T/T_c . The measured velocities agree well with the prediction from two-fluid hydrodynamics [12] combined with the equation of state of the 2D Bose gas [24]. According to the analysis of [12] for weakly interacting gases, the change of speed of sound is mainly due to the variation of the superfluid fraction f_s from ≈ 1 at $T = 0$ to ≈ 0.5 close to $T = T_c$ with the approximate scaling $c_{HD}^{(2)} \propto f_s^{1/2}$ [13]. We note the absence of a discernable discontinuity of sound velocity at T_c, in disagreement with the two-fluid hydrodynamic approach.

In order to explain this disagreement, we first note that collective excitations in ultracold Bose gases can be of different nature depending on the relative amplitude of mean-field effects and collisions between particles [9, 25, 26]. In the very degenerate regime $T \ll T_c$, the system is naturally described within quantum hydrodynamics [27], where interactions between particles occur via a mean-field energy E_{int}. This is valid for $\omega \ll E_{int}/\hbar$, which is satisfied for our setup. In this regime we expect sound waves propagating at c_B, as observed in the experiment. For larger temperatures, but still below T_c, the normal fraction becomes significant. In order to use an hydrodynamic two-fluid model in that case, the local equilibrium condition also requires $\omega \ll \Gamma_{coll}$, where $\Gamma_{coll} = \hbar\tilde{g}^2 n/(2m)$ is the collision rate [28]. The same condition holds for the single fluid case above T_c. The opposite "collisionless" regime has been recently studied in Refs. [29, 30]. It also leads to the existence of a sound mode, originating solely from mean-field interactions described for example by a Landau-Vlasov kinetic equation. For $T \gtrsim T_c$ this collisionless sound mode has a velocity notably smaller than the hydrodynamic result and close to the prediction of Ref. [12] for the second sound velocity at T_c. For our data above T_c we estimate Γ_{coll}/ω to be in the range $1.6 - 3.4$, which indicates that we are in a crossover between these limiting hydrodynamic and collisionless regimes.

The distinction between the quantum hydrodynamics regime and the crossover regime ($\Gamma_{coll} \sim \omega$) is supported by the study of the measured quality factors (see Fig. 3b). For $T \ll T_c$, damping can be described at first order by the decay of low-lying collective excitations via scattering on thermal excitations [15, 31], the so-called Landau damping mechanism. It predicts an increase of the quality factor when decreasing temperature due to the reduction of the number of thermal excitations available for scattering with the sound mode [32]. This perturbative approach is meaningful for large enough quality factors and does not take into account interactions between phonon modes. The solid line in Fig. 3b corresponds to Landau prediction for a 2D system [23]. It shows an overall good agreement with our data, even close to T_c where it gradually looses its validity. Finally, above T_c,

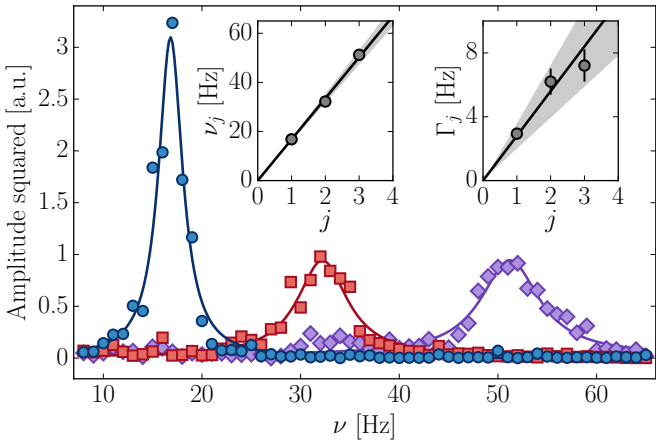

FIG. 4. Observation of standing waves in the box potential. Contribution of the three lowest-energy modes to the amplitude of the density modulation: $j = 1$ (circles), $j = 2$ (squares), $j = 3$ (diamonds). The solid lines are Lorentzian fits. The two insets show the resonance frequencies ν_j and the full widths at half maximum Γ_j resulting from these fits. The solid lines in the insets are linear fit to the data and the shaded areas represent the uncertainty on the fitted slope. From the slope $c/(2L_y)$ of the fit to the resonance frequencies, we find $c = 1.90(9)\,\mathrm{mm/s}$. For this specific experiment, the length of the cloud is $L_y = 57(1)\,\mu\mathrm{m}$ and the degree of degeneracy is $T/T_c = 0.41(7)$.

we measured low quality factors, showing that the observed sound mode are strongly damped, in agreement with the predictions of the collisionless sound mode [29].

In the highly degenerate regime, the low damping rate allows us to observe standing waves. To study them, we modulate sinusoidally the amplitude of the potential creating the dip of density on one edge of the box [33]. After $\approx$1 s we extract, for each frequency ν of the excitation, the amplitude of the (time-dependent) density modulation induced on the cloud (see Ref. [18] for details). We show in Fig. 4 the contribution of the three lowest-energy modes to the amplitude of the modulation as a function of the excitation frequency. For each mode j we observe a clear resonance peak centered at a frequency ν_j. We display in the insets the resonance frequencies and width of the modes. The ν_j's are equally spaced, as confirmed by the linear fit. In addition, the right inset shows the widths of the peaks. They also increase approximately linearly with j [34], meaning that the quality factor associated to these peaks is almost the same, as expected for Landau damping.

We focus in this work on a weakly interacting Bose gas which features a large compressibility compared to liquid helium or strongly interacting Fermi gases. A natural extension of this work would thus be to investigate second sound propagation for increasing interactions [13]. It would also be interesting to investigate first sound, e.g. by applying a localized temperature excitation [5]. During the completion of this work we were informed that a related study with a homogeneous 3D Fermi gas was currently performed at MIT [35].

†Present address: Fakultät für Physik, Ludwig-Maximilians-Universität München, Schellingstr. 4, 80799 Munich, Germany. This work is supported by DIM NanoK and ERC (Synergy UQUAM). This project has received funding from the European Union's Horizon 2020 research and innovation programme under the Marie Skłodowska-Curie grant agreement N° 703926. We thank S. Stringari, L. Pitaevskii, M. Ota, N. Proukakis, F. Dalfovo, F. Larcher and P.C.M. Castilho for fruitful discussions, M. Villiers for experimental assistance and F. Gerbier, R. Lopes and M. Zwierlein for their reading of the manuscript.

J.L.V. and R.S.J. contributed equally to this work.

* beugnon@lkb.ens.fr; †Present address: Fakultät für Physik, Ludwig-Maximilians-Universität München, Schellingstr. 4, 80799 Munich, Germany.

[1] R.J. Donnelly, "The two-fluid theory and second sound in liquid helium," Phys. Today **62**, 34–39 (2009).
[2] S. Balibar, "The discovery of superfluidity," J. Low Temp. Phys. **146**, 441–470 (2007).
[3] E. Taylor, H. Hu, X.-J. Liu, L. P. Pitaevskii, A. Griffin, and S. Stringari, "First and second sound in a strongly interacting Fermi gas," Phys. Rev. A **80**, 053601 (2009).
[4] J. Joseph, B. Clancy, L. Luo, J. Kinast, A. Turlapov, and J. E. Thomas, "Measurement of sound velocity in a Fermi gas near a Feshbach resonance," Phys. Rev. Lett. **98**, 170401 (2007).
[5] L.A. Sidorenkov, M.K. Tey, R. Grimm, Y.-H. Hou, L. Pitaevskii, and S. Stringari, "Second sound and the superfluid fraction in a Fermi gas with resonant interactions," Nature **498**, 78–81 (2013).
[6] A. Griffin and E. Zaremba, "First and second sound in a uniform Bose gas," Phys. Rev. A **56**, 4839–4844 (1997).
[7] A. Griffin, T. Nikuni, and E. Zaremba, *Bose-condensed gases at finite temperatures* (Cambridge University Press, 2009).
[8] M. R. Andrews, D. M. Kurn, H.-J. Miesner, D. S. Durfee, C. G. Townsend, S. Inouye, and W. Ketterle, "Propagation of sound in a Bose-Einstein condensate," Phys. Rev. Lett. **79**, 553–556 (1997).
[9] D.M. Stamper-Kurn, H.-J. Miesner, S. Inouye, M.R. Andrews, and W. Ketterle, "Collisionless and hydrodynamic excitations of a Bose-Einstein condensate," Phys. Rev. Lett. **81**, 500–503 (1998).
[10] R. Meppelink, S. B. Koller, and P. van der Straten, "Sound propagation in a Bose-Einstein condensate at finite temperatures," Phys. Rev. A **80**, 043605 (2009).
[11] Z. Hadzibabic and J. Dalibard, "Two-dimensional Bose fluids: An atomic physics perspective," Rivista del Nuovo Cimento **34**, 389 (2011).
[12] T. Ozawa and S. Stringari, "Discontinuities in the first and second sound velocities at the Berezinskii-Kosterlitz-Thouless transition," Phys. Rev. Lett. **112**, 025302 (2014).
[13] M. Ota and S. Stringari, "Second sound in a two-

dimensional Bose gas: From the weakly to the strongly interacting regime," Phys. Rev. A **97**, 033604 (2018).
[14] D.J. Bishop and J.D. Reppy, "Study of the superfluid transition in two-dimensional ^{4}He films," Phys. Rev. Lett. **40**, 1727–1730 (1978).
[15] L.P. Pitaevskii and S. Stringari, "Landau damping in dilute Bose gases," Phys. Lett. A **235**, 398–402 (1997).
[16] J.L. Ville, T. Bienaimé, R. Saint-Jalm, L. Corman, M. Aidelsburger, L. Chomaz, K. Kleinlein, D. Perconte, S. Nascimbène, J . Dalibard, and J. Beugnon, "Loading and compression of a single two-dimensional Bose gas in an optical accordion," Phys. Rev. A. **95**, 013632 (2017).
[17] M. Aidelsburger, J. L. Ville, R. Saint-Jalm, S. Nascimbène, J. Dalibard, and J. Beugnon, "Relaxation dynamics in the merging of N independent condensates," Phys. Rev. Lett. **119**, 190403 (2017).
[18] "See Supplemental Materials at xxx for methods and complementary results, which includes [36–41],".
[19] N. Prokof'ev, O. Ruebenacker, and B. Svistunov, "Critical point of a weakly interacting two-dimensional Bose gas," Phys. Rev. Lett. **87**, 270402 (2001).
[20] N. Navon, A.L. Gaunt, R.P. Smith, and Z. Hadzibabic, "Emergence of a turbulent cascade in a quantum gas," Nature **539**, 72–75 (2016).
[21] The study of the second spatial mode gives oscillation frequencies that are in good approximation twice larger than the lowest-energy mode and thus results in very similar speeds of sounds. However, the damping rate of this mode is also larger (see Fig. 4) and we cannot robustly estimate its lifetime for our deliberately weak excitation protocol.
[22] The choice of this oscillating function ensures a null derivative of the amplitude of the mode at $t = 0$, when the potential creating the density dip is removed. This behavior is expected from the continuity of the wavefunction and of its derivative describing the state of the gas at $t = 0$.
[23] M.-C. Chung and A.B. Bhattacherjee, "Damping in 2D and 3D dilute Bose gases," New J. Phys. **11**, 123012 (2009).
[24] N. Prokof'ev and B. Svistunov, "Two-dimensional weakly interacting Bose gas in the fluctuation region," Phys. Rev. A **66**, 043608 (2002).
[25] A. Griffin, Wen-Chin Wu, and S. Stringari, "Hydrodynamic modes in a trapped bose gas above the Bose-Einstein transition," Phys. Rev. Lett. **78**, 1838–1841 (1997).
[26] D. Guéry-Odelin, F. Zambelli, J. Dalibard, and S. Stringari, "Collective oscillations of a classical gas confined in harmonic traps," Phys. Rev. A **60**, 4851–4856 (1999).
[27] L. Pitaevskii and S. Stringari, *Bose-Einstein condensation and superfluidity*, Vol. 164 (Oxford University Press, 2016).
[28] D.S. Petrov and G.V. Shlyapnikov, "Interatomic collisions in a tightly confined Bose gas," Phys. Rev. A **64**, 012706 (2001).
[29] M. Ota, F. Larcher, F. Dalfovo, L. Pitaevskii, N.P. Proukakis, and S. Stringari, "Collisionless sound in a uniform two-dimensional Bose gas," arXiv:1804.04032 (2018).
[30] A. Cappellaro, F. Toigo, and L. Salasnich, "Collisionless dynamics in two-dimensional bosonic gases," arXiv:1807.02541 (2018).
[31] R. Meppelink, S. B. Koller, J. M. Vogels, H. T. C. Stoof, and P. van der Straten, "Damping of superfluid flow by a thermal cloud," Phys. Rev. Lett. **103**, 265301 (2009).
[32] Note that Beliaev damping, another mechanism for the decay of low-lying excitations, is absent for the first spatial mode of the box. Indeed, it corresponds to a decay of a low-lying excitation into two excitations with lower energies and thus does not exist for the lowest energy mode.
[33] Y.-H. Wang, A. Kumar, F. Jendrzejewski, R.M. Wilson, M. Edwards, S. Eckel, G.K. Campbell, and C.W. Clark, "Resonant wavepackets and shock waves in an atomtronic SQUID," New J. Phys. **17**, 125012 (2015).
[34] Because of the finite duration of the excitation (1 s), the width of the peaks is Fourier limited at a typical width of 1 Hz, which should be taken into account for a more quantitative analysis.
[35] M. Zwierlein, talk at the BEC 2017 Frontiers in Quantum Gases, Sant Feliu de Guixols.
[36] L. Corman, J. L. Ville, R. Saint-Jalm, M. Aidelsburger, T. Bienaimé, S. Nascimbène, J. Dalibard, and J. Beugnon, "Transmission of near-resonant light through a dense slab of cold atoms," Phys. Rev. A **96**, 053629 (2017).
[37] K. Hueck, N. Luick, L. Sobirey, J. Siegl, T. Lompe, and H. Moritz, "Two-dimensional homogeneous Fermi gases," Phys. Rev. Lett. **120**, 060402 (2018).
[38] A. Ramanathan, S.R. Muniz, K.C. Wright, R.P. Anderson, W.D. Phillips, K. Helmerson, and G.K. Campbell, "Partial-transfer absorption imaging: A versatile technique for optimal imaging of ultracold gases," Rev. Sci. Instrum. **83**, 083119 (2012).
[39] M.F. Riedel, P. Böhi, Y. Li, T.W. Hänsch, A. Sinatra, and P. Treutlein, "Atom-chip-based generation of entanglement for quantum metrology," Nature **464**, 1170 (2012).
[40] V. Pastukhov, "Damping of Bogoliubov excitations at finite temperatures," J. Phys. A: Math. Theor. **48**, 405002 (2015).
[41] P.C. Hohenberg and P.C. Martin, "Microscopic theory of superfluid helium," Ann. Phys. **34**, 291–359 (1965).